

IRIS RECOGNITION IN VISIBLE LIGHT DOMAIN

Daniel Riccio¹ and Maria De Marsico²

¹ *Biometric and Image Processing Laboratory, University of Salerno, via Ponte don Melillo, 84084, Fisciano, Italy*

² *Dipartimento di Informatica, Sapienza Università di Roma, via Salaria 113, 00198, Rome, Italy*

Keywords: Iris Recognition, Linear Binary Pattern, BLOB.

Abstract: Present iris recognition techniques allow very high recognition performances in controlled settings and with cooperating users; this makes iris a real competitor to other biometric traits like fingerprints, with the further advantage of requiring a contactless acquisition. Moreover, most of the existing approaches are designed for Near Infrared or Hyperspectral images, which are less affected by changes in illumination conditions. Current research is focusing on designing new techniques aiming to ensure high accuracy even on images acquired in visible light and in adverse conditions. This paper deals with an approach to iris matching based on the combination of local features: Linear Binary Patterns (LBP) and discriminable textons (BLOBs). Both these technique have been readapted in order to deal with images captured in variable visible light conditions, and affected by noise due to distance/resolution or to scarce user collaboration (blurring, off-axis iris, occlusion by eyelashes and eyelids). The obtained results are quite convincing and strongly motivate the addition of more local features.

1 INTRODUCTION

In controlled settings and with cooperative users, iris provides comparable or even higher accuracy than other biometric traits like fingerprints. Therefore, present research trend is towards focusing on the possibility of relaxing some of the strong constraints for subject cooperation and the quality of the acquired image. An iris based recognition system working in every-day applications has to deal with several kinds of distortions, such as blurring, off-axis, occlusions and reflections. As a matter of fact, in a semi-controlled setting, due either to lower user's cooperation, or to limited performances of the capture device, the system must work over noisy iris images, which are often partially compromised.

Literature offers a wide spread of iris based techniques for automatic personal identification (Bowyer, 2008). The first, significant work about iris recognition was presented in 1993 by J. Daugman (Daugman, 1993), whose approach relied on an integro-differential filter to locate the useful region, and on 2D Gabor filters to extract relevant features. Wildes' (Wildes, 1997) proposal was quite different: an edge detection filter during segmentation, and then Hough transform to detect circular regions. The feature extraction process

constructs a Laplacian pyramid by iteratively applying a Gaussian lowpass filter and decimation operator to the iris image. The similarity between new samples and stored templates is computed using the normalized correlation. Both these systems (Daugman and Wildes) require a strict image quality control to guarantee a high identification accuracy, as they are heavily influenced by illumination and position changes.

In (Sung, 2002) the authors discuss potential issues to be overcome in order to make an iris identification algorithm working in uncontrolled settings. They specifically address the off-angle and defocused images problems by proposing *ad hoc* correction algorithms, while the illumination problem is considered insurmountable, unless input images are acquired with special lighting equipments. In (Du, 2005), Du *et al.* investigated about the use of three different kinds of partial iris recognition (left-to-right, outside-to-inside, inside-to-outside). In their experiments, the authors concluded that only the inner part of the iris is really discriminating. In (Dorairaj, 2005), Dorairaj *et al.* described a strategy to correct off-angle images before extracting the biometric features. They start with the estimation of the gaze direction and then apply a projective transformation bringing the captured iris image to frontal view. Recently, other

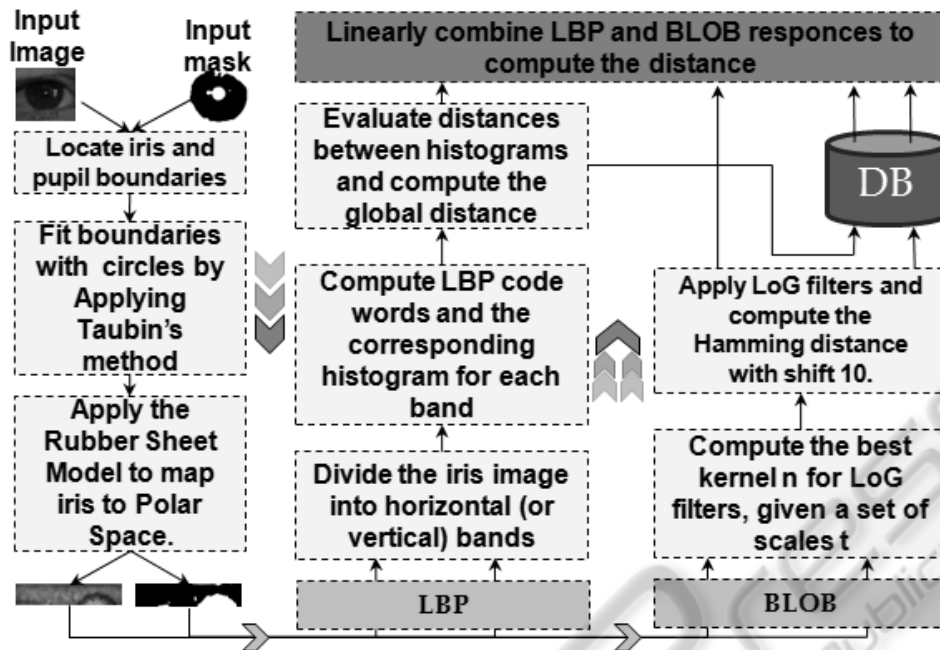


Figure 1: The architecture of N-IRIS.

researchers including (Proença, 2007) and (Bower, 2008) have contributed new methods to decrease the effects of lighting conditions and low quality captured images. Despite this, most of them expect a cooperative behaviour from the user. This implicit assumption represents a strong limitation for all those settings not guaranteeing this requirement. In present research non-cooperative iris recognition is still a great challenge.

Many approaches try to solve these problems by working locally, by analyzing separate iris sub-regions independently. Along this line, a Noisy Iris Recognition Integrated Scheme (N-IRIS) is proposed in this paper (Figure 1).

It adopts and combines two local feature extraction techniques, Linear Binary Patterns (LBP) and extraction of discriminable textons (BLOBs), which differently and independently characterize relevant regions of iris.

In order to be effectively applied to iris recognition, the proposed local operators must provide a low computational cost. Iris recognition systems often acquire high resolution images or have to work in real time. The LBP descriptor meets this requirement, although providing a discriminating local texture descriptor, since it seems to be the best-able for quite regular patterns. However, the uniqueness of the iris texture is also characterized by the irregular distribution of local feature blocks such as *furrows*, *crypts* and *freckles* or *spots*. Such features can be considered as *blobs*: a group of

image pixels which form a structure which can be darker or lighter than the surrounding region. The extraction of the blobs from an iris image is obtained through different LoG (Laplacian of Gaussian) filter banks. This technique will be referred as BLOB.

Both LBP and BLOB have been adapted to the case at hand. Further, their combination has also been investigated. The fusion between the two approaches is performed at score level by exploiting a weighted mean of matching scores. Experimental results show that such combination of the LBP and BLOB, though not particularly complex, overcomes both single strategies in terms of accuracy. This suggests that different kinds of iris features may call for different suited codings for a better matching. Possible future studies will focus on the combination of more kinds of features, as well as the design of more sophisticated schemes for the integration of different information.

2 IMAGE SEGMENTATION

Typically an iris identification system starts with the location and segmentation of the iris sample. The precision of the separation between the useful region for identification and those that can be considered as noise elements (reflections, eyelids, eyelashes) heavily influence subsequent steps. The higher such precision, the more informative the obtained iris code, and therefore the better the expected

recognition result.

The *collarete* separates the two main parts of the iris that are the *pupillary* and *ciliary* regions. The former is the innermost one and determines the pupil's contour, while the latter is the outermost one and surrounds the pupillary region. *Sclera*, *eyelids* and *eyelashes* represents further important elements, which are taken into account during segmentation as well as coding. As a matter of fact, eyelids and eyelashes may often hinder a correct segmentation, and may lead to a poor coding if they are included in the pupil code. On the other hand, useful structures for recognition are crypts, circular and radial furrows, freckles and spots with various extent.

Though strictly correlated, according to the preceding considerations, segmentation and matching represent two well distinguishable steps. International challenges like NICE also performed such kind of distinction, since NICE I explicitly and uniquely addressed the problem of noisy iris segmentation, while NICE II focused on the problem of matching noisy iris images. However, methods participating to the NICE II competition have been provided with segmentation mask produced by the best performing segmentation algorithm (Tan, 2010) in previous NICE I (Figure 2 shows some examples). N-IRIS exploits such segmentation mask to refine and transform the iris region into a rectangular region, from which features are then extracted.

N-IRIS starts by approximating iris and pupil boundary by circumferences (centre and radius) as accurately as possible, so as to allow the mapping from the image Cartesian space to the iris region polar space. Possible distortion introduced in this phase invalidate all the following steps. In a naïve solution both circumferences are approximated by solving an ellipse fitting problem. However, Figure 2 (b) shows some cases in which such approach fails to retrieve the desired circumferences. This happens because the ellipse fitting algorithm is too sensible to discontinuities introduced in the iris and pupil contours by occlusions due to reflections or eyelids. In practice, curves resulting from contour approximation tend to get completely deformed just to precisely adhere to the available boundary portion. A further problem arises in all those cases which are similar to the irises in the third row of Figure 2: the black region contour represents a single object without discontinuities. This makes it difficult to distinguish pupil frontier points from iris contour ones.

A more articulated solution is then needed to cope with problems caused by images like that in the third

row of figure 2. The segmentation algorithm implemented in N-IRIS locates the pupil contour first, and proceeds by separating the pupil from the iris region. The mask is scanned row by row from top to bottom. Each row is scanned from the first to the last column, by marking the first and the last black pixels. These pixels represent the iris frontier. Frontier points are inputted to the Taubin's algorithm that approximates planar curves through implicit equations (more details on this method are discussed in (Taubin, 1991)) and outputs the centre and radius of the circumference representing the iris.

A new circle centred in the iris centre, but with a radius length of 1/5 of the iris radius is considered (pupil will most likely fall inside this zone) and all image pixels which fall outside such circle are deleted. The centre and the radius of the circumference approximating the pupil are determined by repeating the procedure of circle fitting on this new image, after inverting it.

Since the iris often undergoes several kinds of distortions due to the illumination conditions, to the acquisition distance or to partial occlusions, before proceeding to actual feature extraction, one needs to transform the iris region in a suitable form, also considering future matching operations. Capture distance represents a potential issue, as the iris diameter may not be constant and the iris shape influences matching results. Therefore, this dimension must be normalized, yet avoiding to lose details or to introduce "ghost" information and also taking into account possible translations and rotations. Furthermore, illumination conditions cause dilation/contraction and small displacements of the pupil that is seldom exactly located at the center of the iris. Therefore N-IRIS transforms the iris so that the iris representation is constant in dimensions and that relevant features are approximately located in the same points. To this aim the Rubber Sheet Model by Daugman (Daugman, 1993, Daugman, 2004) is exploited. This model maps the iris in radial coordinates while fixing the final dimensions of the obtained (rectangular) image. Due to anticipated scarce resolution of iris images at hand, N-IRIS adopts a radial resolution (number of pixels along a radial line) of 40 pixels, and an angular resolution (number of radial lines around the iris region) of 360 pixels. The same normalization is separately performed on the segmentation mask associated to each image (Figure 3). The mask is such that $M(x,y)=1$ if $I(x,y)$ is a pixel of noise, and $M(x,y)=0$ otherwise, so that only information in relevant iris regions is coded.

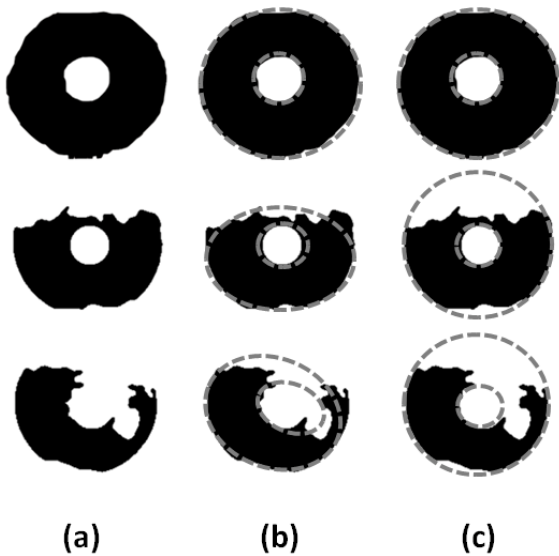


Figure 2: Column (a) shows, from top to bottom, iris masks of increasing difficulty; column (b) shows mask processing by ellipse fitting; column (c) shows mask processing by N-IRIS.

3 FEATURE EXTRACTION

The feature extraction process aims to generate a discriminating code for the iris annulus after that noisy elements (e.g. eyelashes, which occupy different positions and extent in different captures of the same subject) have been discarded by the segmentation algorithm. The quite rich structure of the iris texture suggests to adopt different local operators to capture different kinds of salient information, while a subsequent fusion algorithm merges their matching results at the score level. The present work only exploits binary patterns to record textural regularities present in the iris, and blob identification for coding lighter or darker spots inside the iris region (Figure 3). However, future developments will investigate the addition of appropriate versions of further local operators.

In particular, the first attempts were aimed at investigating the usefulness of local texture analysis based on Local Binary Pattern (LBP) (Ojala, 2002, Mäenpää, 2000). In particular, the solution in (Sun, 2006) has been evaluated, before devising a proprietary version, based on experimental evidence on the best strategy to be adopted. In order to further enhance the obtained results, this *ad hoc* implementation of the LBP was combined with a blob identification strategy (Chenhong, 2008), namely BLOB. The BLOB algorithm has been further enhanced to extract discriminable textons,

representing image regions which are lighter or darker than the surrounding zone. Then, N-IRIS merges the matching criteria stemming from the two techniques, to exploit the respective strengths.

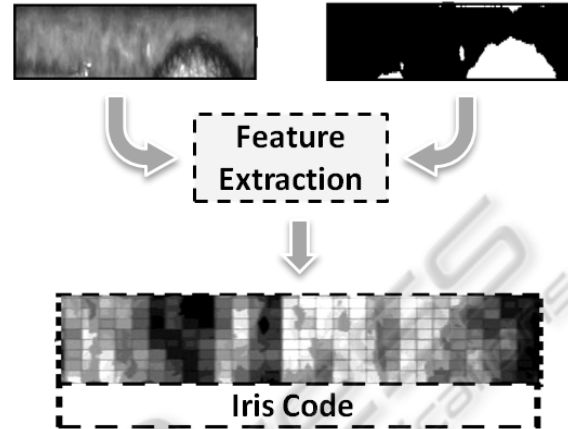


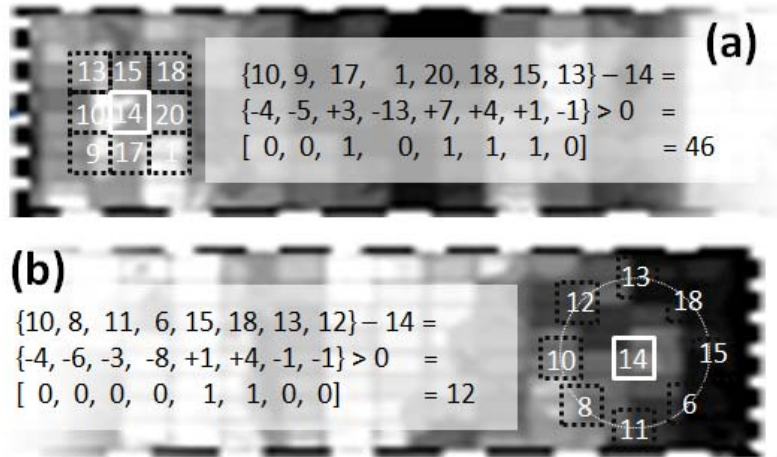
Figure 3: Feature extraction and coding based on normalized iris image and segmentation mask.

3.1 Linear Binary Pattern

The Local Binary Pattern (LBP) is a local operator introduced by Ojala (Ojala, 2002) to analyze image texture. In its basic version, the operator evaluates the 3×3 square region surrounding a pixel (eight neighbours). Each neighbour has a corresponding position in a 8 bits string, so that if the central pixel has a lower value than one of its neighbours, a 1 is recorded in the string for such neighbour, and a 0 otherwise (Figure 4). A variation is presented by (Ojala, 2002), where the basic operator is extended to process pixel neighbourhoods of variable dimension, and to be invariant to rotations. The circular neighbourhood of a pixel is exploited, and sample points are identified by interpolation. The resulting operator is called $LBP_{P,R}$ where P is the number of sample points, and R is the radius of the neighbourhood.

Sun *et al.* re-adapted LBP for iris recognition (Sun, 2006). Their approach divides the normalized iris image into blocks (Figure 5 (a)) and computes an histogram for each of them. N-IRIS further improves Sun's method with a less computationally expensive solution. N-IRIS splits the normalized iris image into horizontal (or vertical) bands b_j (Figure 5 (b) and (c)) and computes the histogram H_j of LBP values for each of them. The overall iris code C is built up by concatenating all histograms H_j and the noise mask M : $C=(H_1, H_2, \dots, H_{bands}, M)$.

N-IRIS assumes that the mask M is provided by the segmentation algorithm. The mask M is used


 Figure 4: Computation of LBP (a) and LBP_{PR} (b).

during matching to take into account the amount of noise which is present within the compared bands. The higher the number of noise pixels in the matched bands, the less reliable the similarity measure between the histograms.

Given two codings $C_1=(H_1, H_2, \dots, H_{bands}, M)$ and $C_2=(K_1, K_2, \dots, K_{bands}, N)$, and any histogram similarity measure δ (e.g. correlation, intersection or Bhattacharyya), matching is performed by computing the mean of the following values:

$$\delta(H_b, K_b) \cdot \left(1 - \frac{\overline{noise}_b}{totpixel}\right), \forall b \in \{1, 2, \dots, bands\} \quad (1)$$

where \overline{noise}_b represents the mean number of noise pixels in the b -th band of masks M and N . Bands specialize blocks: a generic block is m (rows) \times n (columns) pixels, an horizontal band is a $1 \times n$ block and a vertical band is a $m \times 1$ block. Once blocks are ordered row-first, formula (1) always holds.

Section 4 reports the most significant experiments with LBP on the UBIRIS.v2, which were aimed to testing both different types (block, vertical, horizontal) and numbers of bands. Results suggested that five horizontal bands represent the best choice, which mostly depends on the normalization parameters. It is also interesting to notice that the most accurate solution in terms of type of bands is also the most bound to anatomical features, since horizontal bands in the polar image correspond to circular bands in the original image, and therefore are expected to be quite significant in coding iris features.

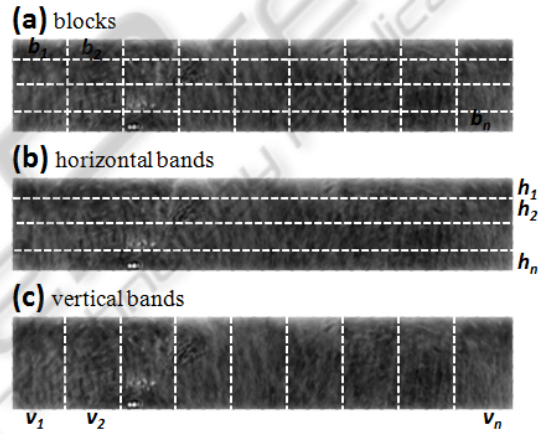


Figure 5: Division in (a) blocks, (b) horizontal bands, (c) vertical bands.

3.2 BLOB

What we call BLOB is a differential operator combining a Laplacian operator (a good contour detector, but very sensible to noise) with a Gaussian filter (to preliminarily smooth the image). It is very effective in identifying lighter or darker regions in the iris (Figure 6). N-IRIS improves the basic BLOB method in (Chenhong, 2008) with a better blob setting off, due to increased size of the Gaussian filter. In that work blobs are modelled by a Gaussian 2-dimensional non-symmetric function, with length features $\sqrt{t_1}$ and $\sqrt{t_2}$:

$$f(x_1, x_2) = g(x_1, t_1)g(x_2, t_2) = \frac{e^{-\frac{x_1^2}{2t_1} - \frac{x_2^2}{2t_2}}}{2\pi\sqrt{t_1 t_2}} \quad (2)$$

To identify blobs of different sizes, the

representation must be given both in space and in scale. For the semi-group property of Gaussian kernels $g(\cdot; t_A) * g(\cdot; t_B) = g(\cdot; t_A + t_B)$ the authors derive:

$$L = g(x_1; t_1 + t)g(x_2; t_2 + t) \quad (3)$$

If an image undergoes a space-scale smoothing, values of spatial derivatives generally decrease with scale. Then a normalized differential operator ∇_{norm}^2 must be used. The authors show that the normalized response of a blob detector at scale t is:

$$\nabla_{norm}^2 L = t(\nabla^2 L) \quad (4)$$

The solution by (Chenhong, 2008) to extract and code blob features is: fix the different scales, compute $\nabla_{norm}^2 L$ for each scale and fuse the results by taking, for each pixel, the maximum value among all scales. Popular computational tricks allow to fuse Gaussian and Laplacian in a single LoG operator. Here the sizes of the convolution kernels at different scales were found using cross-validation, e.g. regression.

N-IRIS computes a matrix with real coefficients, where positive values correspond to dark spots, while negative values represent light ones. A threshold operation is applied to binarize those values: negative values are set to 0, while positive ones are mapped on 1. Matching between two binary codes can be performed by Hamming distance, weighted by the segmentation masks, as discussed by (Daugman, 1993). In order to account for rotation variations, N-IRIS also considers shifts of 10 pixels and returns as the final distance, the one computed on the alignment returning the maximum match. A further improvement has been attempted by chaining the separate scale (binary) codings in a longer code, instead of fusing them. Matching was performed by comparing codes at the same scale and taking the mean of obtained values as distance. This modality will be referred as *chain*, as opposed to the original one (*fusion*). It seemed to rely on more discriminative information, but this did not produce the expected improvements.

3.3 Combining LBP and BLOB

LBP and BLOB methods have been combined according to a parallel protocol. This results in a multi-classifier approach referred to as LBP-BLOB. The iris biometric key is made up by chaining LBP and BLOB codes. When two iris biometric keys have to be matched, LBP and BLOB work separately and fusion is performed at score level. Given I a normalized iris image and M its

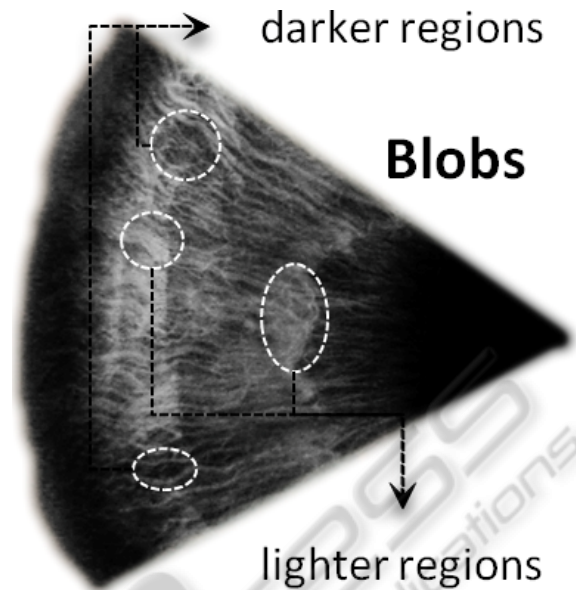


Figure 6: Some examples of *blobs* that are local features such as *furrows*, *crypts* and *freckles* or *spots*.

normalized segmentation mask, N-IRIS computes c_{LBP} and c_{BLOB} , the LBP and BLOB coding of the couple (I, M) respectively (actually, coding is only performed on the I element). Thus, the final method for coding and matching is:

- Coding of the pair (I, M) is $c = \{c_{LBP}, c_{BLOB}\}$
 - Matching between codings c_1 and c_2 is given by:
- $$\delta(c_1, c_2) = \lambda \delta_{LBP}(c_{1,LBP}, c_{2,LBP}) + (1 - \lambda) \delta_{BLOB}(c_{1,BLOB}, c_{2,BLOB}), \quad (5)$$

where the value 0.5 for λ was found experimentally. The adopted fusion strategy was assessed by experiments on a large set of iris images. On this sufficiently substantial test bed, it was observed that LBP and BLOB show a quite uncorrelated behaviour in terms of ability to discriminate between genuine and impostor matches.

Though this is not a formal proof of the actual lack of correlation between the two techniques, it is an expected result considered that they rely on different theoretical frameworks, aiming to capture different relevant characteristics (texture regularity and the presence of significant "hot spots"). In future research lines, a related study represents a core point. For the time being, the previous observations can explain, in the present setting, why the simple sum of the two scores improves the performances of the single classifiers, as confirmed by experimental results.

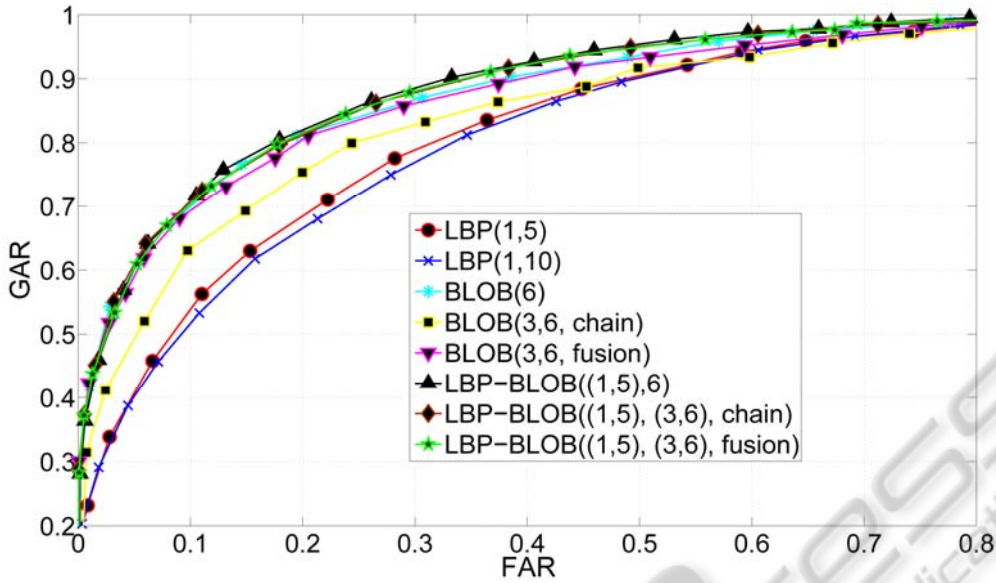


Figure 7: Results from LBP, BLOB and LBP-BLOB with different configurations on NICE II tuning database.

4 EXPERIMENTAL RESULTS

The experiments to assess N-IRIS performances were performed on the database of 1000 images and corresponding segmentation masks provided for tuning purposes by NICE II program committee to challenge participants, together with a dedicated JAVA platform. The results were measured in terms of the classical accuracy "figure of merit" Receiving Operating Curve (ROC).

All color images were converted in gray scale by assigning each pixel the weighted mean of the three primary channels of its RGB color. LBP was tested by dividing the images in horizontal or vertical bands and in blocks. $LBP(n,m)$ will denote LBP execution on an image subdivided in n columns and m rows. BLOB was run in single scale configuration, with fusion of different scale results, and with chaining (see Section 3.2). Scale t varied in the set $T=\{2,4,6,8,12,16,24\}$. In *fusion* and *chain* modes, pairs (t_1, t_2) and triplets (t_1, t_2, t_3) of scales from T have been considered. $BLOB(t_1)$ will denote single scale execution of BLOB at scale t_1 , $BLOB(t_1, t_2, mode)$ will denote the execution of BLOB in mode $mode \in \{chain, fusion\}$ for the pair of scales (t_1, t_2) and $BLOB(t_1, t_2, t_3, mode)$ will denote the execution of BLOB in mode $mode \in \{chain, fusion\}$ for the triplet of scales (t_1, t_2, t_3) . A configuration for LBP-BLOB combines single configurations for LBP and BLOB: $LBP-BLOB(n, m, t_1)$, $LBP-BLOB(n, m, t_1, t_2, mode)$ and $LBP-BLOB(n, m, t_1, t_2, t_3, mode)$.

Figure 7 shows the ROC curves from LBP and

BLOB with different configurations, as well as different combinations of such configurations, on UBIRIS v2. The subdivision in five horizontal bands seems an optimal LBP configuration for this databases. BLOB in *fusion* mode (the original one) provides better results than BLOB in *chain* mode. Moreover, BLOB works better with a single scale on UBIRIS.v2. Though sounding strange, this is a consequence of the scarce clearness of most images in this database. For such images, using more scales provides poor benefit. BLOB seems to perform better than LBP, but this trend is reversed on low resolution images. This underlines a better ability by LBP to extract relevant features in these cases. It is worth noticing that normalization fails in some critical situations, were the useful iris region is especially scarce and, at the same time, iris and pupil boundaries are not well separated as in the last row of Figure 2. Matching problems encountered with LBP are related to excessive blurring, since the histogram undergoes a substantial alteration, while BLOB problems are related to irises with high off-axis angles which significantly alter blobs shape.

Figure 7 also shows that the LBP-BLOB performs better than the single methods. The performances of the combined method were also measured in terms of decidability value. Decidability is defined as a function of mean and variance of intra- and inter-class scores. The higher the index, the better the discrimination ability of the system. If D^I and D^E denote the set of similarities resulting from intra- and inter-class matches, $\mu(D^I)$ and $\mu(D^E)$

the respective mean values, and $\sigma(D^I)$ and $\sigma(D^E)$ the standard deviations, the decidability index is:

$$d = \frac{|\mu(D^I) - \mu(D^E)|}{\sqrt{0.5(\sigma(D^I)^2 + \sigma(D^E)^2)}} \quad (6)$$

On the given dataset, the method achieved a decidability value of 1.4825. N-IRIS was then tested by the NICE II evaluation commission on new images and masks, never provided before. The obtained result is very close to the decidability reported here. It has been submitted to NICE II international competition and has been awarded as one of the best 6 iris segmentation and recognition algorithms (Nice II, 2011).

5 CONCLUSIONS

This work presents an approach for matching irises captured in the visible light spectrum and in uncontrolled settings. Linear Binary Patterns (LBP) and BLOB have been adapted and combined in an original and specific way, to address the difficult operational conditions due to the strongly relaxed capture constraints. The obtained results are quite satisfactory both in terms of ROC and of decidability value, most of all against the present research scenario, as the independent tests performed by NICE II program committee have demonstrated. This is a strong motivation to further improve performances. A very promising research line is the use of more local features, able to set off different iris peculiarities, as for example the directionality of extracted patterns.

REFERENCES

- Bowyer K. W., Hollingsworth K., Flynn P. J., 2008. Image Understanding for Iris Biometrics: A Survey, vol. 110, no. 2, pp. 281–307.
- Chenhong L., Zhaoyang L., 2008. Local feature extraction for iris recognition with automatic scale selection. *Image and Vision Computing*, vol. 26, no. 7, pp. 935–940.
- Daugman J., 2004. How Iris Recognition Works, *IEEE Transactions on Circuits and Systems for Video Technology*, vol. 14, no. 1, pp. 21–30.
- Daugman, J., 1993. High confidence visual recognition of persons by a test of statistical independence. *IEEE Transactions Pattern Analysis and Machine Intelligence* vol. 15, no. 11, pp. 1148-1161.
- Dorairaj V., Schmid N., Fahmy G., 2005. Performance evaluation of non-ideal iris based recognition system implementing global ICA encoding. *In Proceedings of the IEEE International Conference on Image Processing (ICIP 2005)*, pp. 285–288.
- Du Y., Bonney B., Ives R., Etter D., Schultz R., 2005. Analysis of partial iris recognition using a 1-d approach. *In Proceedings of the IEEE International Conference on Acoustics, Speech and Signal Processing (ICASSP'05)*, pp. 961–964.
- Ojala T., Pietikäinen M., Mäenpää T., 2002. Multiresolution gray-scale and rotation invariant texture classification with local binary patterns. *IEEE Transactions on Pattern Analysis and Machine Intelligence*, vol. 24, no. 7, pp. 971–987.
- Proença H., Alexandre L. A., 2007. Toward non-cooperative iris recognition: A classification approach using multiple signatures,” *IEEE Transactions on Pattern Analysis and Machine Intelligence*, vol. 9, no.4, pp. 607–612.
- Proença H., Filipe S., Santos R., Oliveira J., Alexandre L. A., 2010. The UBIRIS.v2: A Database of Visible Wavelength Images Captured On-The-Move and At-A-Distance, *IEEE Transactions on Pattern Analysis and Machine Intelligence*, vol. 32, no. 8, pp. 1529–1535.
- Sun Z., Tan T., Qiu X., 2006. Graph Matching Iris Image Blocks with Local Binary Pattern. *In Proceedings of the International Conference on Biometrics*, pp.366–372
- Sung E., Chen. Xilin, Yang J., 2002. Towards non-cooperative iris recognition systems. *In Proceedings of the seventh International Conference on Control, Automation, Robotics and Vision*, pp. 990–995.
- Tan T., Hea Z., Sun Z., 2010. Segmentation of Visible Wavelength Iris Images Captured At-a-distance and On-the-move, *Image and Vision Computing*, vol. 28, no. 2, pp. 223–230.
- Taubin G., 1991. Estimation Of Planar Curves, Surfaces And Nonplanar Space Curves Defined By Implicit Equations, With Applications To Edge And Range Image Segmentation. *IEEE Transaction on Pattern Analysis and Machine Intelligence*, vol. 13, pp. 1115–1138.
- Mäenpää T., Ojala T., Pietikäinen M., Soriano M., 2000. Robust Texture Classification by Subsets of Local Binary Patterns. *15-th International Conference on Pattern Recognition*, pp. 947–950.
- Wildes R., 1997. Iris recognition: an emerging biometric technology. *Proceedings of the IEEE*, vol. 85, no. 9, 1997.
- NICE II, nice2.di.ubi.pt. Last visit on November 06 2011.